Some new results on stability of incommensurate fractional systems and their $\mathscr{L}_p$-norms

Rachid MALTI
Université de Bordeaux – IMS UMR 5218 CNRS, France
Email: firstname.lastname@ims-bordeaux.fr

***Abstract*—Stability of fractional systems is yet an open problem especially when dealing with incommensurate differentiation orders. The objective of the invited talk is twofold. First of all, a new method [1] for determining stability regions, in the parametric space, of fractional incommensurate systems is presented. It is based on interval arithmetics and allows, beyond the stability property, to specify the regions in the parametric space that have the same number of unstable poles. Hence, all transfer functions which parameters belong to the same stability region have the same stability property.**

Contrary to rational systems, the stability property of fractional systems does not guarantee the existence (or the boundedness) of the $\mathscr{L}_p$-norms, $1 \leq p \leq \infty$, of their impulse response. Hence, the second objective of the talk is to examine the existence conditions of these $\mathscr{L}_p$-norms [2]. The established results are used to choose a performance index for evaluating stable feedback control system performances.

I. Introduction

Fractional systems has been attracting a lot of interest during the last two decades in different fields of engineering and science, since the seminal work by Oldham and Spanier [3], [4] for modeling diffusive phenomena.

Fractional systems can be described in transfer function form:

$$F(s) = \frac{\sum_{i=0}^{M} b_i s^{\beta_i}}{1 + \sum_{j=1}^{N} a_j s^{\alpha_j}} \tag{1}$$

where the exponents of s can be ordered $0 < \alpha_1 < \alpha_2 < \ldots < \alpha_N$, $0 \leq \beta_0 < \beta_1 \ldots < \beta_M$ and $(a_i, b_j) \in \mathbb{R}^2, \forall i = 0, 1, \ldots, M, \forall j = 1, 2, \ldots, N$. The multivalued function $s \mapsto s^\nu$ becomes holomorphic in the complement of its branch cut line of the complex plane, chosen to be along the negative real axis, $\mathbb{R}_{\leq 0}$, including the branching points 0 and ∞. Hence, $F(s)$ is a meromorphic function in the complement of $\mathbb{R}_{\leq 0}$ of the complex plane: $\mathbb{C} \setminus \mathbb{R}_{\leq 0}$.

The $\mathscr{L}_p$-norm of $f(t)$, the impulse response of $F(s)$, is defined as[1]

$$\begin{cases} \|f\|_p = \sqrt[p]{\int_0^{+\infty} |f(t)|^p \, dt} & \text{for } 1 \leq p < \infty \\ \|f\|_\infty = \sup\limits_{t \in \mathbb{R}_{\geq 0}} |f(t)| \end{cases} \tag{2}$$

[1]Note that $f(t)$ is a continuous-time function and hence the supremum is used instead of the essential supremum in the definition of $\|f\|_\infty$.

A function $f(t)$ is said to belong to the Lebesgue space $\mathscr{L}_p(\mathbb{R}_{\geq 0})$ with $p \in [1, \infty]$, or $\mathscr{L}_p$ in short, if its p-norm is finite: $\|f\|_p < \infty$.

The system $F(s)$ is $\mathscr{L}_p$-stable, $1 \leq p \leq \infty$, if and only if:

$$\sup_{u \in \mathscr{L}_p, u \neq 0} \frac{\|f \star u\|_p}{\|u\|_p} < \infty \tag{3}$$

where $\star$ stands for the convolution product and $u(t)$ the system input. Condition (3) is satisfied, $\forall p \in [1, \infty]$, when

$$f \in \mathscr{L}_1(\mathbb{R}_{\geq 0}) \tag{4}$$

In such a case:

$$\|f \star u\|_p < \|f\|_1 \|u\|_p \tag{5}$$

The bounded-input-bounded-output (BIBO) stability is defined as the $\mathscr{L}_\infty$-stability.

Due to its simplicity, the most used criterion for testing stability of fractional systems is Matignon's theorem [5, theorem 2.21]. It allows deciding whether a system is stable by locating its s^ν-poles. It generalizes the classical Routh-Hurwitz criterion for rational systems. It is extended to take into account variations of $\nu \in (0, \infty)$ in [6].

Theorem 1. *A commensurate transfer function, of order ν, $F(s) = \frac{T(s^\nu)}{R(s^\nu)}$, where T and R are coprime polynomials, is BIBO-stable if and only if*

$$0 < \nu < 2 \tag{6}$$

and for every $s \in \mathbb{C}$ such that $R(s) = 0$

$$|\arg(s)| > \nu \frac{\pi}{2} \tag{7}$$

However, Matignon's theorem applies only for stability checking of commensurate fractional systems. When the system is incommensurate, some other criteria, mainly based on Cauchy's principal theorem [7] or its derivatives such as the Nyquist theorem [8] are used. However, these methods are quite difficult to implement in practice.

Since (4) is only a necessary condition, the system might be $\mathscr{L}_p$-stable and yet have an impulse response, f, with an infinite $\mathscr{L}_p$-norm $\forall p \in [1, \infty]$. This feature is not common in the classical rational systems: when a rational system is $\mathscr{L}_p$-stable then its $\mathscr{L}_p$-norms are finite.

II. Stability of uncommensurate fractional systems

This section of the paper contains results of a joint work with Milan R. Rapai'c and Vukan Turkulov, which is currently submitted at the ICFDA'2021 conference [1].

Bonnet and Partington [9] proved that $F(s)$ is BIBO-stable if and only if it is analytic in the right-half complex plane $\{\mathscr{Re}(s) \geq 0\}$. In such a case

$$F(s) \in \mathscr{H}_\infty(\mathbb{C}_+) \tag{8}$$

where $\mathscr{H}_\infty(\mathbb{C}_+)$ is the Hardy space of analytic functions on the open right-half plane $\mathbb{C}_+$.

On the other hand, it can be proven from Rouché's theorem that all system poles vary continuously with its parameters anywhere in the complex-plane except the branch-cut, $\mathbb{R}_{\leq 0}$. Moreover, when transfer function differentiation orders vary, new poles can appear or vanish only on the branch-cut. Hence, the basic idea is to consider that if a fractional system is stable for a given parametric point then it remains stable unless its poles cross the imaginary axis. Further, assuming that there is no possible simplification between poles and zeros of $F(s)$ in (1), the stability of $F(s)$ depends only on the position of the zeros of the characteristic function:

$$\bar{f}(s, \boldsymbol{\alpha}) = 1 + \sum_{j=1}^{N} a_j s^{\alpha_j} \tag{9}$$

A. Problem formulation

According to the previous remarks, the following problems can be formulated in the parametric space:

(P1) Finding stability and instability regions. In this case, the objective is to check whether, for positive $\boldsymbol{\alpha} \in \mathbb{R}^n_{\geq 0}$, $\bar{f}(\rho e^{j\theta}, \boldsymbol{\alpha})$ has zeros in the right half complex plane including the imaginary axis. However, due to the symmetry of complex conjugate zeros, the searching domain can be restreint to the first quadrant of the complex s-plane: $(\rho, \theta) \in \mathbb{R}_{\geq 0} \times \left[0, \frac{\pi}{2}\right]$.

(P2) Finding the Stability Crossing Sets (SCS) between stability and the instability regions. In this case, the searching domain in the complex plane is restraint to $(\rho, \theta) \in \mathbb{R}_{\geq 0} \times \{\frac{\pi}{2}\}$. Hence, only values of $\boldsymbol{\alpha} \in \mathbb{R}^n_{\geq 0}$, for which the poles are crossing the imaginary axis towards the instability region are searched for.

Hence, the problems (P1) and (P2) can be formulated as finding the set of all feasible parameters

$$\boldsymbol{\theta} = (\rho, \theta, \boldsymbol{\alpha})^T \in \Omega = \left(\mathbb{R}_{\geq 0} \times \Theta \times \in \mathbb{R}^n_{\geq 0}\right), \tag{10}$$

where $\Theta = \left[0, \frac{\pi}{2}\right]$ for (P1) and $\Theta = \left\{\frac{\pi}{2}\right\}$ for (P2), satisfying

$$\begin{cases} \mathscr{Re}\{\bar{f}(\rho e^{j\theta}, \boldsymbol{\alpha})\} = 0 \\ \quad \text{and} \\ \mathscr{Im}\{\bar{f}(\rho e^{j\theta}, \boldsymbol{\alpha})\} = 0 \end{cases} \tag{11}$$

If $\exists \boldsymbol{\theta} = (\rho, \theta, \boldsymbol{\alpha})^T \in \Omega$ such that $\bar{f}(\rho e^{j\theta}, \boldsymbol{\alpha}) = 0$, then, for the problem (P1), the characteristic function has zeros in the closed right half complex plane and, for the problem (P2), on the imaginary axis, which allows determining the SCS.

Both of these problems can be formulated as a Constraint Satisfaction Problem $\mathcal{CSP}$[2]

$$\mathcal{CSP}: \begin{cases} \mathscr{Re}\{\bar{f}(\rho e^{j\theta}, \boldsymbol{\alpha})\} = 0 \\ \mathscr{Im}\{\bar{f}(\rho e^{j\theta}, \boldsymbol{\alpha})\} = 0 \\ 0 < \rho < \mathcal{R}, \quad \theta \in \Theta, \\ \alpha \in \mathbb{R}^n_{\geq 0} \end{cases} \tag{12}$$

where $\mathcal{R}$ is ∞ in theory and is finite in practice for evident implementation reasons. The solution set $\mathbb{S}$ for the problem (12) is rewritten as:

$$\mathbb{S} = \{\boldsymbol{\theta} \in \Omega \mid \mathscr{Re}\{\bar{f}(\rho e^{j\theta}, \boldsymbol{\alpha})\} \subset [0] \text{ and } \mathscr{Im}\{\bar{f}(\rho e^{j\theta}, \boldsymbol{\alpha})\} \subset [0]\}. \tag{13}$$

The characterization of the whole set $\mathbb{S}$ can be formulated as a set inversion problem:

$$\mathbb{S} = f^{-1}([0]) \cap \Omega, \tag{14}$$

and solved by guaranteed methods using interval arithmetics, introduced in the next subsection.

B. Introduction to interval arithmetics

Interval analysis was initially introduced by Moore [10]. An interval $[x] = [\underline{x}, \overline{x}]$ is a closed, bounded, and connected set of real numbers. The set of all intervals is denoted by $\mathbb{IR}$. Real operations are extended to intervals as follows. Given $[x] \in \mathbb{IR}$ and $[y] \in \mathbb{IR}$:

$$[x] + [y] = [\underline{x} + \underline{y}, \overline{x} + \overline{y}], \tag{15}$$

$$[x] - [y] = [\underline{x} - \overline{y}, \overline{x} - \underline{y}], \tag{16}$$

$$[x] \times [y] = [\min(\underline{x}\underline{y}, \underline{x}\overline{y}, \overline{x}\underline{y}, \overline{x}\overline{y}), \max(\underline{x}\underline{y}, \underline{x}\overline{y}, \overline{x}\underline{y}, \overline{x}\overline{y})] \tag{17}$$

$$[x]/[y] = \begin{cases} [x] \times \left[\frac{1}{\overline{y}}, \frac{1}{\underline{y}}\right], & \text{if } 0 \notin [y] \\ (-\infty, \infty), & \text{if } 0 \in [y]. \end{cases} \tag{18}$$

Interval arithmetics do not define an algebra because $(\mathbb{IR}, +)$ is not a group. Indeed, elements of $\mathbb{IR}$ do not have an inverse. Take for instance $A = [-1, 1] \in \mathbb{IR}$, then $A + (-A) = [-2, 2]$ is not equal to the degenerated interval $[0] = [0, 0] = \{0\}$. Either, $(\mathbb{IR}, +, *)$ is not a ring etc. Additionally, arithmetic operations on intervals introduce often pessimism because the result of each operation must be included in an interval.

[2]Usually a $\mathcal{CSP}$ is formulated using inequalities

$$\mathcal{CSP}: \begin{cases} \underline{x} \leq \mathscr{Re}\{\bar{f}(\rho e^{j\theta}, \boldsymbol{\alpha})\} \leq \overline{x} \\ \underline{y} \leq \mathscr{Im}\{\bar{f}(\rho e^{j\theta}, \boldsymbol{\alpha})\} \leq \overline{y} \\ 0 < \rho < \mathcal{R}, \quad \theta \in \Theta, \\ \alpha \in \mathbb{R}^n_{\geq 0}, \end{cases}$$

where $\underline{x}, \overline{x}, \underline{y}, \overline{y}$ can also be set to small enough values $-\epsilon, \epsilon, -\epsilon, \epsilon$; as in the fourth initialization of the example in section II-E5.

C. Solving the $\mathcal{CSP}$

1) Contractors: The $\mathcal{CSP}$ (12) is solved by a contractor $\mathcal{C}$, which is an operator which permits to reduce the domain $[\boldsymbol{\theta}]$ without any bisection. Hence, contracting the box $[\boldsymbol{\theta}]$ means replacing it by a smaller box $[\boldsymbol{\theta}]^*$ such that the solution set $\mathbb{S}$ remains unchanged, i.e. $\mathbb{S} \subset [\boldsymbol{\theta}]^* \subset [\boldsymbol{\theta}]$ [11]. There exists different types of contractors depending on whether the system to be solved is linear or not.

In our study, a non linear type contractor named *forward-backward contractor* is used to reduce the initial searching space. The basic idea when implementing this contractor is to decompose a principal constraint into primitive constraints. Each primitive constraint involves elementary operators and functions such as $\{+, -, \times, /, \exp, \log, \ldots\}$. The next example illustrates how a given constraint is used to contract a domain.

2) Example: Consider the constraint:

$$\begin{cases} f(\mathbf{x}) = x_3 - x_2 x_1 = 0, \\ x_1 \in [2, 10],\ x_2 \in [1, 10],\ x_3 \in [1, 5], \end{cases} \tag{19}$$

which can be rewritten as:

$$x_3 = x_2 x_1.$$

The forward interval constraint propagation removes all inconsistent values from $[x_3]$ as follows:

$$[x_3] = ([x_1] \times [x_2]) \cap [x_3] = [2, 5].$$

Then, the backward interval constraint propagation removes all inconsistent values from x_1 and x_2 as follows:

$$[x_1] = ([x_3]/[x_2]) \cap [x_1] = [2, 5],$$
$$[x_2] = ([x_3]/[x_1]) \cap [x_2] = [1, 5/2].$$

After a forward and a backward propagation, the contracted box is $[\mathbf{x}] = \big([2, 5], [1, 5/2], [2, 5]\big)^T$ which contains the solution of the $\mathcal{CSP}$.

In some cases the contractor cannot reduce enough the parameters domain. In such cases, bisection of the variable vector $\boldsymbol{\theta}$ is necessary. The algorithm SIVIA [12], which is described in the following section is based on the association of contractors and splitting.

D. Set Inversion Via Interval Analysis (SIVIA)

This algorithm, proposed by Jaulin and Walter in [12], allows to obtain an inner $\underline{\mathbb{S}}$ and an outer $\overline{\mathbb{S}}$ enclosures of the solution set $\mathbb{S}$ (if it exists), such that:

$$\underline{\mathbb{S}} \subseteq \mathbb{S} \subseteq \overline{\mathbb{S}}. \tag{20}$$

SIVIA is a recursive algorithm based on partitioning of the parameter set into three regions: feasible, undeterminate and unfeasible. SIVIA uses an inclusion test $[t] : \mathbb{IR} \to \mathbb{N}$ which is a function allowing to prove if an interval $[\boldsymbol{\theta}]$ is feasible in which case it is added to the set $\underline{\mathbb{S}}$. Any undetermined region is bisected and tested again, unless its size $w([\boldsymbol{\theta}])$ is less than a precision parameter η tuned by the user and which ensures that the algorithm terminates after a finite number of iterations. The outer approximation is then computed as $\overline{\mathbb{S}} = \underline{\mathbb{S}} \cup \Delta\mathbb{S}$ where $\Delta\mathbb{S}$ is the union of all remaining undetermined boxes. Hence, the SIVIA algorithm is presented in algorithm 1.

Algorithm SIVIA (in: $[t], [\boldsymbol{\theta}], \eta$; out: $\underline{\mathbb{S}}, \overline{\mathbb{S}}$)

1) Option: Call contractor on $\boldsymbol{\theta}$.
2) If $[t]([\boldsymbol{\theta}]) = [0]$, return;
3) If $[t]([\boldsymbol{\theta}]) = [1]$, then $\underline{\mathbb{S}} := \underline{\mathbb{S}} \cup [\boldsymbol{\theta}]; \overline{\mathbb{S}} := \overline{\mathbb{S}} \cup [\boldsymbol{\theta}]$, return;
4) If $w([\boldsymbol{\theta}]) \leq \eta, \overline{\mathbb{S}} := \overline{\mathbb{S}} \cup [\boldsymbol{\theta}]$;
   Else bisect $[\boldsymbol{\theta}]$ into $[\boldsymbol{\theta}_1]$ and $[\boldsymbol{\theta}_2]$;
5) SIVIA (in: $[t], [\boldsymbol{\theta}_1], \eta$; out: $\underline{\mathbb{S}}, \overline{\mathbb{S}}$);
6) SIVIA (in: $[t], [\boldsymbol{\theta}_2], \eta$; out: $\underline{\mathbb{S}}, \overline{\mathbb{S}}$).

Algorithm 1: The algorithm

The option in line 1 allows either to call the contractor or not at each execution of the SIVIA algorithm which complexity is known to be exponential!

E. Example

Consider the following transfer function having two differentiation orders.

$$F(s, \boldsymbol{\alpha}) = \frac{1}{s^{\alpha_2} + 2s^{\alpha_1} + 1}, \tag{21}$$

where $\boldsymbol{\alpha} = (\alpha_1, \alpha_2) \in \mathcal{A}_1 \times \mathcal{A}_2 \subset \mathbb{R}^2_{\geq 0}$, $\mathcal{A}_1$ and $\mathcal{A}_2$ define the searching domains. It can be analyzed by checking the position of the zeros of the characteristic function

$$f(s, \boldsymbol{\alpha}) = s^{\alpha_2} + 2s^{\alpha_1} + 1 \tag{22}$$

$$\bar{f}(\rho e^{j\theta}, \boldsymbol{\alpha}) = \rho^{\alpha_2} \cos(\theta\alpha_2) + 2\rho^{\alpha_1} \cos(\theta\alpha_1) + 1 + \mathrm{j}\,(\rho^{\alpha_2} \sin(\theta\alpha_2) + 2\rho^{\alpha_1} \sin(\theta\alpha_1)) \tag{23}$$

1) Implementing the forward-backward contractor on the system under study: A first contractor could be implemented, after the real part of $\bar{f}$:

$$\mathscr{R}e\{\bar{f}(\rho e^{j\theta}, \boldsymbol{\alpha})\} = 0 \Leftrightarrow \rho^{\alpha_2} \cos(\theta\alpha_2) + 1 = -2\rho^{\alpha_1} \cos(\theta\alpha_1) \tag{24}$$

A second one could also be implemented, after the imaginary part of $\bar{f}$:

$$\mathscr{I}m\{\bar{f}(\rho e^{j\theta}, \boldsymbol{\alpha})\} = 0 \Leftrightarrow \rho^{\alpha_2} \sin(\theta\alpha_2) = -2\rho^{\alpha_1} \sin(\theta\alpha_1) \tag{25}$$

However, handling sin and cos functions in each contractor is not an easy task because asin and acos functions return angles in their principal determination, i.e. between 0 and π for the acos, and between $-\frac{\pi}{2}$ and $\frac{\pi}{2}$ for the asin. In that case, care must be taken to set back the angles to the correct determination. Another alternative, is to combine (24) and (25) to obtain another contractor with less sin and cos functions. Such a contractor, named *combined contractor*, is obtained by squaring both equations and summing them up

$$\rho^{2\alpha_2} + 2\rho^{\alpha_2} \cos(\theta\alpha_2) + 1 = 4\rho^{2\alpha_1}. \tag{26}$$

```
function [x]=Comb_Contractor_Red(x)
 global nb_siv;
 xx = x;
 rho = x(1); theta = x(2);
 alpha1 = x(3); alpha2 = x(4);
%Forward
 x1 = rho^(2*alpha2);
 x2 = 2*rho^alpha2;
 x3 = theta*alpha2;
 x4 = cos(x3);
 x5 = x2*x4;
 x6 = x1 + x5 + 1;
 x7 = 4*rho^(2*alpha1);
%Backward
 x7    = intersect(x6, x7);
 alpha1= intersect(alpha1,1/2*log(x7/4)/log(rho));
 rho   = intersect(rho, (x7/4)^(1/(2*alpha1)));
 x6    = intersect(x6, x7);
 x5    = intersect(x5, x6 - x1 - 1);
 x2    = intersect(x2, x5/x4);
 alpha2= intersect(alpha2, log(x2/2)/log(rho));
 rho   = intersect(rho, (x2/2)^(1/alpha2));
 x1    = intersect(x1, x6 - x5 - 1);
 rho   = intersect(rho, x1^(1/(2*alpha2)));
 alpha2= intersect(alpha2, log(x1)/(2*log(rho)));

 x = [rho, theta, alpha1, alpha2];
 if any(isnan(x))
     x=xx;
 end
end
```

Fig. 1. The implementation of the combined contractor (26) using the IntLab toolbox [13] under Matlab.

A single cos function remains in (26) instead of two in the previous two contractors, which is easier to handle. This contractor is implemented in Fig.1, using the IntLab toolbox [13] under Matlab.

The algorithm is applied to the characteristic function (22), using four different initializations. In the first three, the problem (P2) is considered and in the fourth, the problem (P1) is treated.

2) First initialization: The initial searching box and tolerance are respectively set to:

$$\boldsymbol{\theta} = (\rho, \theta, \alpha_1, \alpha_2)^T \in [0,4] \times \left\{\frac{\pi}{2}\right\} \times [0,3] \times [0,4.5] \quad (27)$$

$$\eta = \text{diam}(\boldsymbol{\theta})/2^7 \quad (28)$$

where $\text{diam}(\boldsymbol{\theta})$ defines the length of each element of $(\boldsymbol{\theta})$.

The SIVIA algorithm is executed:

- without contractors (without step 1 in the algorithm). In this case the SIVIA function is called 13 543 times in 190 sec. The obtained outer enclosure $\overline{\mathbb{S}}$ is plotted in Fig.2.
- with the combined contractor (26) called at each step of the SIVIA algorithm (with step 1 in the algorithm). The SIVIA function is called 8 711 times in 296 sec. The obtained outer enclosure $\overline{\mathbb{S}}$ is plotted in Fig.3.

Moreover, the values at which the poles cross the imaginary axis correspond more or less exactly in both cased to the plot of Fig.4, which validates *a posteriori* that all the poles are inside the searching interval $\rho \in [0,4]$. In case some poles were touching the limit $\mathcal{R} = 4$, it would have been necessary to choose a bigger $\mathcal{R}$.

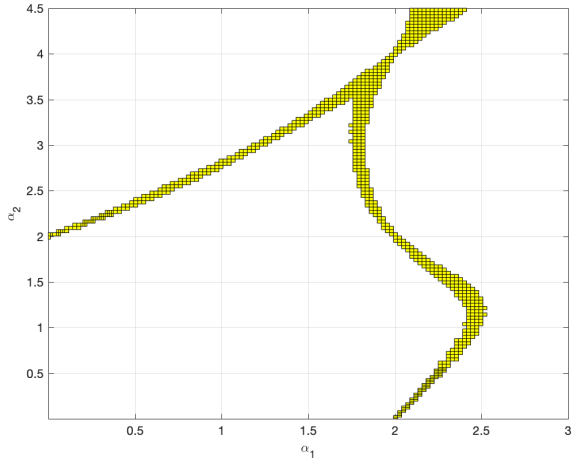

Fig. 2. First initialisation – Stability crossing sets obtained **without contractors**. Zeros of the characteristic function f which arguments equal $\frac{\pi}{2}$ are probably contained in the yellow boundary (outer enclosure $\overline{\mathbb{S}}$). The lower left region delimited by the yellow boundary represents the guaranteed stability region.

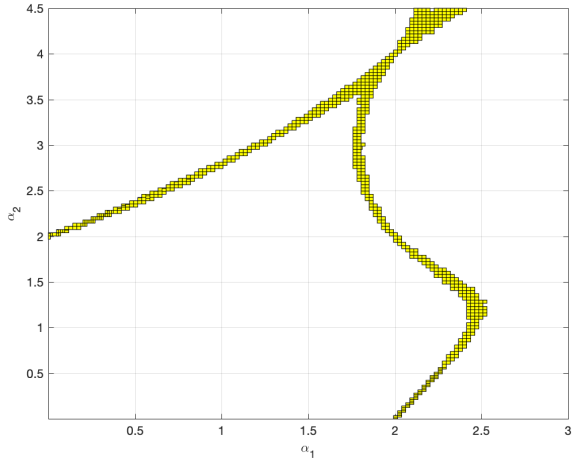

Fig. 3. The same as Fig.2, however **with contractors**.

As a conclusion, regarding this first initialization, the algorithm using the combined contractor is a little bit more precise for the same tolerance factor η. Execution speeds of both algorithms are comparable. The former as compared to the latter converges in a bigger number of iterations, however quicker, because the latter calls the contractor at each SIVIA iteration.

3) Second initialization: Let's search for the SCS by enlarging the searching domain. The initial box is now set to:

$$\boldsymbol{\theta} = (\rho, \theta, \alpha_1, \alpha_2)^T \in [0,4] \times \left\{\frac{\pi}{2}\right\} \times [0,15] \times [0,20] \quad (29)$$

The tolerance is defined as in (28), however applied to the new definition of the initial searching box.

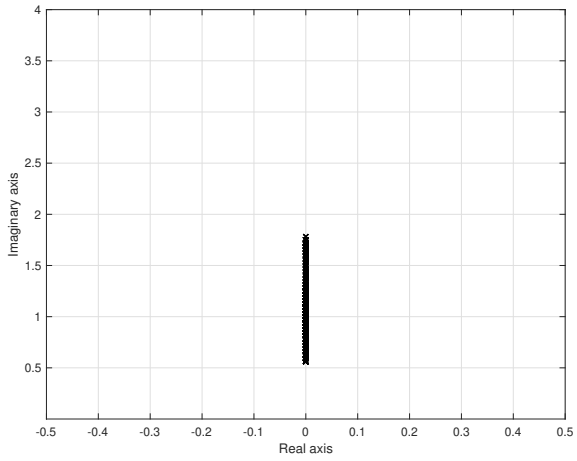

Fig. 4. First initialization – Zeros of the characteristic function $\bar{f}$ crossing the imaginary axis.

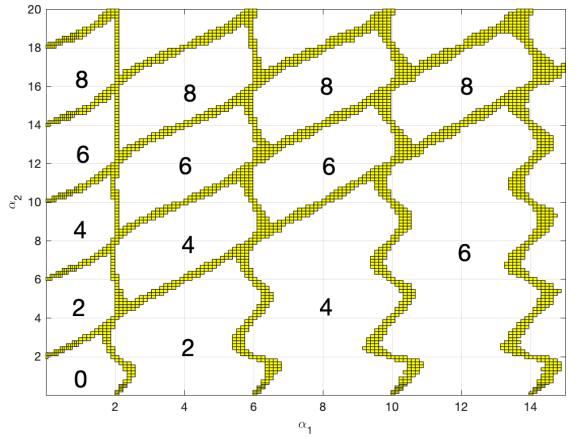

Fig. 5. Second initialization – Stability Crossing Sets (wider intervals as compared to Figs.2 and 3). The number of unstable poles is indicated in each region.

The SIVIA algorithm, without contractors, is called 73 037 times in 1 090 seconds. The obtained outer enclosure $\overline{\mathbb{S}}$ of the SCS is plotted in Figs 5, which indicates additionally the number of unstable poles, computed at integer values of the parametric points. Hence, all systems with parameters inside the different regions delimited by the SCS have the indicated number of poles. The intervals of poles look very much like the ones in Fig.4.

4) Third initialization: A major change is operated here. Instead of testing, the $\mathcal{CSP}$ defined in (12), a new $\mathcal{CSPN}$ is defined by enlarging the acceptable mapping of $\bar{f}(\rho e^{j\theta}, \boldsymbol{\alpha})$ to a square of size ϵ instead of a single point (the origine).

$$\mathcal{CSPN}: \begin{cases} -\epsilon \leq \mathscr{R}e\{\bar{f}(\rho e^{j\theta}, \boldsymbol{\alpha})\} \leq \epsilon, \\ -\epsilon \leq \mathscr{I}m\{\bar{f}(\rho e^{j\theta}, \boldsymbol{\alpha})\} \leq \epsilon, \\ 0 < \rho < \infty, \quad \theta \in \Theta, \\ 0 < \alpha_1 < \infty, \ 0 < \alpha_2 < \infty, \\ \epsilon = 0.1 \end{cases} \tag{30}$$

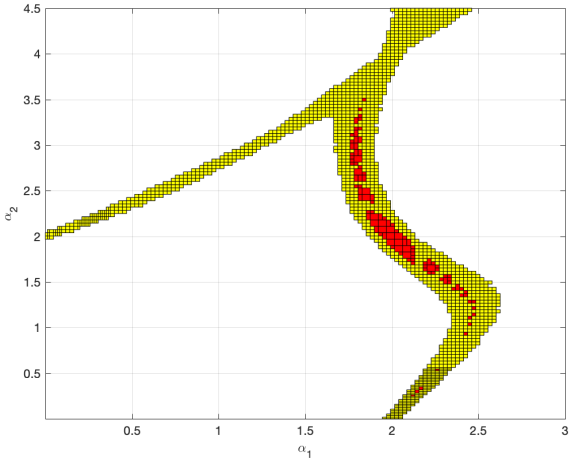

Fig. 6. Third initialization – Inner $\underline{\mathbb{S}}$ (in red), and Outer $\overline{\mathbb{S}}$ (in yellow) enclosures of the $\mathcal{CSPN}$ defined in (30)

Hence, instead of searching for the zeros of the characteristic function $\bar{f}$ in (22), the algorithm searches for intervals $[\boldsymbol{\theta}]$ that are mapped according to $\bar{f}$ inside a square of length ϵ. This is the usual way $\mathcal{CSP}$s are formulated. The same parameters and tolerance are chosen as in the first initialization in (27) and (28).

The results, obtained without contractors in 27 795 iterations and 443 sec, are plotted in Fig.9, where red and yellow parts indicate the inner and the outer enclosures $\underline{\mathbb{S}}$ and $\overline{\mathbb{S}}$ of (20).

It turns out not to be interesting to consider the $\mathcal{CSPN}$ (30) instead of the initial $\mathcal{CSP}$ (12), because it widens the feasible solution set as the square, of length ϵ, defining the admissible mapping gets wider.

5) Fourth initialization: In this part, the problem (P1) is solved. Hence, instead of looking for the stability crossing sets, let's look for all the zeros of $\bar{f}(\rho e^{j\theta}, \boldsymbol{\alpha})$ in the first quadrant. Consider the $\mathcal{CSP}$ in (12), and the following searching box:

$$\boldsymbol{\theta} = (\rho, \theta, \alpha_1, \alpha_2)^T \in [0, 4] \times \left[0, \frac{\pi}{2}\right] \times [0, 3] \times [0, 4.5] \tag{31}$$

When setting the tolerance to (28), the algorithm is stopped after an hour because of convergence issues. Then, the tolerance is augmented to:

$$\eta = \text{diam}(\boldsymbol{\theta})/2^4$$

The algorithm converges in 12 525 iterations and 194 sec. The obtained outer enclosure $\overline{\mathbb{S}}$ is plotted in Fig.7.

Apparently, the root-searching-domain in the first quadrant, is validated *a posteriori* in Fig.8: all the poles of the first quadrant are inside the searching domain, defined by $\rho \in [0, 4]$, when $(\alpha_1, \alpha_2) \in \times[0, 3] \times [0, 4.5]$.

Higher precision is definitely required to find out a better sketch of the stability region (in white).

However, this problem appears to be ill-posed as the $\mathcal{CSP}$ (12) evaluated for interval values of $[\boldsymbol{\theta}]$, can never be satisfied. A mapping of $[\boldsymbol{\theta}]$ with $\bar{f}$ is an interval that can never be a subset of $\{0\}$. Hence, in the instability region, the algorithm

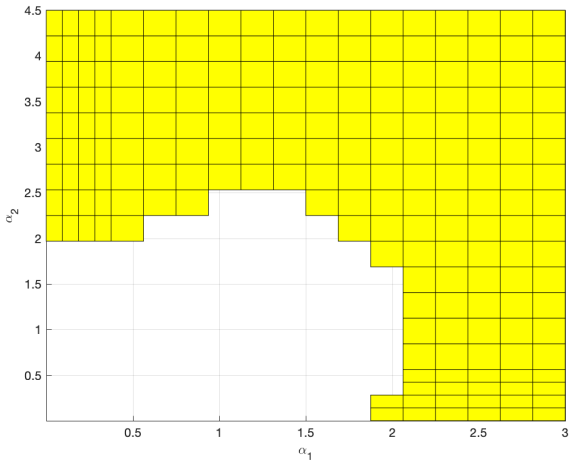

Fig. 7. Fourth initialization – Guaranteed stability in white and possible instability (outer enclosure $\overline{\mathbb{S}}$) in yellow

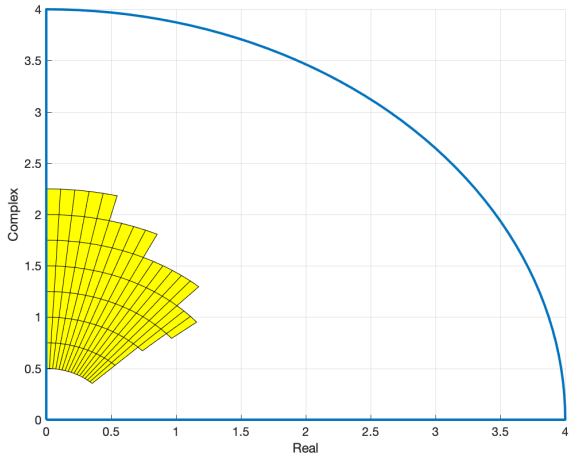

Fig. 8. Fourth initialization – Possible root location in yellow, searching domain boundary in blue

will keep bisecting, until reaching the precision η. It turns out that the time complexity of the SIVIA algorithm is higher than a brute-force search on boxes of elementary sizes η, which is not interesting.

As a conclusion of this part, it turns out that it is more interesting to solve the problem (P2) by looking for the stability crossing sets and deducing the stability regions.

III. Which norm for fractional systems?

This section of the paper contains results originally published in [2].

As mentioned previously, (4) is only a necessary condition. The system might be $\mathscr{L}_p$-stable and yet have an impulse response, f, with an infinite $\mathscr{L}_p$-norm $\forall p \in [1, \infty]$. The following theorem, proven in [2], states the existence conditions of the $\mathscr{L}_p$-norms.

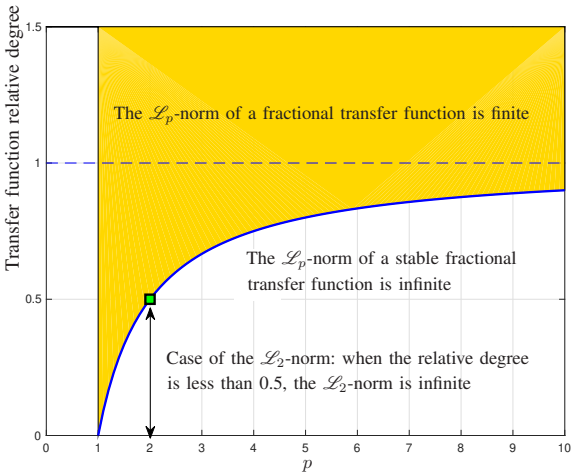

Fig. 9. Finiteness region of the $\mathscr{L}_p$-norm of fractional stable transfer functions in the relative-degree versus p plane. The border curve $(1 - \frac{1}{p})$ does not belong to the finiteness region.

Theorem 2. *Let a fractional transfer function as*

$$\tilde{F}(s) = \frac{F(s)}{s^{\mu}} \tag{32}$$

where $F(s)$, given by (1), is BIBO-stable and where $\mu \geq 0$. Numerator and denominator of $F(s)$ are assumed to be coprime (with no possible simplification between poles and zeros). Then, the $\mathscr{L}_p$-norm, $1 \leq p \leq \infty$, of the impulse response of $\tilde{F}(s)$ is finite if and only if the transfer function relative degree satisfies:

$$\mu + \alpha_N - \beta_M > 1 - \frac{1}{p} \tag{33}$$

and the integrator order satisfies:

$$0 < \mu < 1 - \frac{1}{p} \tag{34}$$

or

$$\mu = 0 \tag{35}$$

The yellow zone in Fig.9 shows finite combinations of $\mathscr{L}_p$-norms, in the plane relative-degree versus p. Similarly, the orange zone in Fig.10 shows finite combinations of $\mathscr{L}_p$-norms, in the plane integrator-order versus p.

Remarks:

- $\mathscr{L}_p$-norm finiteness conditions (33)-(34) are in accordance with the $\mathscr{L}_2$-norm finiteness conditions determined in [14].
- Equation (33) shows that all the $\mathscr{L}_p$-norms of rational systems, $\forall 1 \leq p \leq \infty$, are always finite because the relative degree is an integer at least equal to one (for a proper transfer function with no nonzero feedthrough gain). Additionally, (34) shows that the $\mathscr{L}_p$-norms, $\forall 1 \leq p \leq \infty$, are always infinite in presence of a rational integrator, with $\mu = 1$.
- A pure integrator $\frac{1}{s^{\mu}}$, $\forall \mu \in \mathbb{R}_{>0}$, has always an infinite $\mathscr{L}_p$-norm, $\forall 1 \leq p \leq \infty$, because conditions $\mu + \alpha_N -$

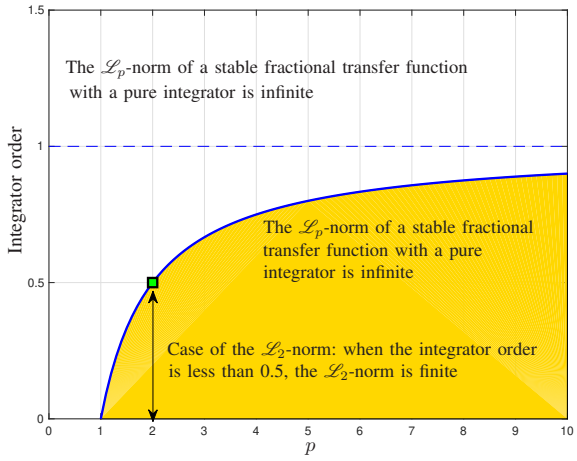

Fig. 10. Finiteness region of the $\mathscr{L}_p$-norm of fractional stable transfer functions in the integrator-order versus p plane. The border curve $(1-\frac{1}{p})$ does not belong to the finiteness region, except the point $(p=1, \mu=0)$ which does.

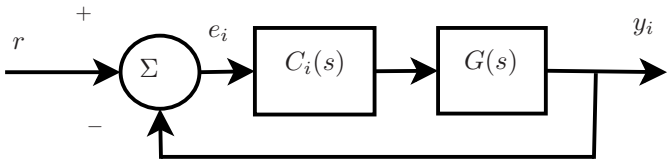

Fig. 11. A simple feedback control system structure

$\beta_M > (1-\frac{1}{p})$ and $\mu < (1-\frac{1}{p})$, cannot be satisfied simultaneously (here $\alpha_N = \beta_M = 0$) .

In the following example, the results are used to choose a proper criterion for evaluating performance of a feedback control loop.

IV. Example

This example is taken from [15, example 2]. Consider the simple feedback control system structure of Fig.11 and different fractional order PI controllers, with $i \in \{1,2,3,4\}$,

$$C_i(s) = K_{p_i} + \frac{K_{I_i}}{s^{\lambda_i}}, \tag{36}$$

which yield different closed-loop transfer functions:

$$T_i(s) = \frac{C_i(s)G_i(s)}{1+C_i(s)G_i(s)} \tag{37}$$

as reported in Table 1. Tavazoei (2010) evaluates numerically different integral performance indices among which the integral of absolute error (IAE) and the integral of squared error (ISE), on a step response. The IAE and ISE-indices are respectively the $\mathscr{L}_1$-norm and the $\mathscr{L}_2$-norm squared of the error signal $e_i(t)$ of Fig.11 (respectively $\|e_i\|_1$ and $\|e_i\|_2^2$) when the input $r(t)$ is a step:

$$E_i(s) = \frac{1}{s}(1-T_i(s)) \tag{38}$$

The $\mathscr{L}_2$-norm of $e_i(t)$ was also computed analytically in [14] and allowed to confirm the results announced in [15] regarding the ISE-index. In this paper, the $\mathscr{L}_4$-norm of $e_i(s)$ is additionally computed by numerical integration of the time-domain signals $e_i(t)$. The $\mathscr{L}_\infty$-norm is deduced easily.

Note that $E_1(s)$ has a proper integrator of order 0.2 and hence, according to (34), an infinite $\mathscr{L}_1$-norm and finite $\mathscr{L}_p$-norms for $p > 1.25$. Consequently, $\|e_i\|_2, \|e_i\|_4$, and $\|e_i\|_\infty$ are finite. $E_4(s)$ has a proper integrator of order 0.5 and hence infinite $\mathscr{L}_1$ and $\mathscr{L}_2$-norms. Additionally, [15] has evaluated other performance indices such as the *integral of time multiplied absolute error* (ITAE), the *integral of time multiplied squared error* (ITSE), and the *integral of squared of time multiplied error* (ITSE). All these performance indices were shown to be infinite for $E_4(s)$. No finite performance index has been proposed in [15] for evaluating the output feedback control law for $E_4(s)$. Theorem 2 and condition (34) show that the $\mathscr{L}_p$-norm is finite for all $p > 2$. Here, the $\mathscr{L}_4$-norm of the error signal can be used as a finite performance index of the output feedback control. For the remaining systems, $E_2(s)$ and $E_3(s)$ have no integrators, relative degrees greater than $(1-\frac{1}{p})$, stable $s^{0.5}$-poles, and hence finite $\mathscr{L}_p$-norms $\forall 1 \leq p \leq \infty$. Note that $\|e_i\|_\infty$ equals 1 for all i, because the step response always starts at $y_i(0) = 0$ and hence $\|e_i\|_\infty = e_i(0) = 1$. Consequently, the $\mathscr{L}_\infty$-norm is not, in this case, an interesting performance index.

V. Conclusions

This paper proposes an algorithm, based on interval arithmetics, for stability analysis of fractional transfer functions. Guaranteed stability region is determined in the parametric space. Two problems have been formulated and it has been shown that the problem of finding the parametric region for which the system is unstable is ill-posed because the bisection algorithm has a time-complexity worse than a brute-force search. However, the problem of finding stability crossing sets turns out to be very interesting, as it allows finding with a reasonable complexity, the stability crossing sets and hence deducing the whole stability region.

Having stable fractional transfer functions does not, however guarantee the existence of the $\mathscr{L}_p$-norms of its impulse response. Some additional conditions on its relative degree must be fulfilled. This helps choosing a performance criterion for feedback control loops.

The analytical computation of the $\mathscr{L}_2$-norm was proposed in [14] for commensurate systems only. A challanging task would be to extend this result to incommensurate systems.

References

[1] R. Malti, M. R. Rapaić, and V. Turkulov, "Stability analysis of incommensurate elementary fractional systems using interval arithmetics," in *International Conference on Fractional Differentiation and its Applications (ICFDA)*, Warsaw, Poland, 2021.

[2] R. Malti, "A note on L_p-norms of fractional systems," *Automatica*, vol. 49, no. 9, pp. 2923–2927, 2013. [Online]. Available: http://www.sciencedirect.com/science/article/pii/S0005109813003166

[3] K. Oldham and J. Spanier, "The replacement of Fick's laws by a formulation involving semi-differentiation," *Electro-anal. Chem. Interfacial Electrochem*, vol. 26, pp. 331–341, 1970.

[4] ——, *The fractionnal calculus - Theory and Applications of Differentiation and Integration to Arbitrary Order*. Academic Press, New-York and London, 1974.

i	$T_i(s)$	$E_i(s)$	$\|e_i\|_1$-IAE	$\|e_i\|_2^2$-ISE	$\|e_i\|_4^4$	$\|e_i\|_\infty$
1	$\frac{2s^{0.8}+1}{2s^{2.4}+s^{1.6}+s^{0.8}+1}$	$\frac{2s^{1.6}+s^{0.8}-1}{2s^{2.6}+s^{1.8}+s+s^{0.2}}$	∞	3.43	2.28	1
2	$\frac{2s^{1.6}+s^{0.8}+1}{2s^{2.4}+s^{1.6}+s^{0.8}+1}$	$\frac{2s^{1.4}-s^{0.6}}{2s^{2.4}+s^{1.6}+s^{0.8}+1}$	3.48	1.10	0.27	1
3	$\frac{s^{1.6}+s^{0.8}+1}{2s^{2.4}+s^{1.6}+s^{0.8}+1}$	$\frac{2s^{1.4}}{2s^{2.4}+s^{1.6}+s^{0.8}+1}$	3.32	1.11	0.35	1
4	$\frac{2s^{0.5}+1}{2s^{1.5}+s+s^{0.5}+1}$	$\frac{2s+s^{0.5}-1}{2s^{2}+s^{1.5}+s+s^{0.5}}$	∞	∞	0.27	1

TABLE I

$\mathscr{L}_1, \mathscr{L}_2, \mathscr{L}_4$, AND $\mathscr{L}_\infty$,-NORMS OF $e_i(t)$ FOR DIFFERENT OUTPUT FEEDBACK CONTROL SYSTEMS TAKEN FROM (TAVAZOEI, 2010, EXAMPLE 2).

[5] D. Matignon, "Stability properties for generalized fractional differential systems," *ESAIM proceedings - Systèmes Différentiels Fractionnaires - Modèles, Méthodes et Applications*, vol. 5, 1998.

[6] R. Malti, X. Moreau, F. Khemane, and A. Oustaloup, "Stability and resonance conditions of elementary fractional transfer functions," *Automatica*, vol. 47, no. 11, pp. 2462–2467, 2011.

[7] C. Hwang and Y.-C. Cheng, "A numerical algorithm for stability testing of fractional delay systems," *Automatica*, vol. 42, no. 5, pp. 825 – 831, 2006.

[8] J. Trigeassou, A. Benchellal, N. Maamri, and T. Poinot, "A frequency approach to the stability of fractional differential equations," *Transactions on Systems, Signals & Devices (TSSD)*, vol. 4, no. 1, pp. 1 – 25, 2009.

[9] C. Bonnet and J. Partington, "Coprime factorizations and stability of fractional differential systems," *Systems & Control Letters*, vol. 41, no. 3, pp. 167 – 174, 2000.

[10] R. Moore, *Interval analysis*. Englewood Cliffs, NJ: Prentice-Hall, 1966.

[11] L. Jaulin, M. Kieffer, O. Didrit, and E. Walter, *Applied interval analysis*. London: Springer-Verlag, 2001.

[12] L. Jaulin and E. Walter, "Set inversion via interval analysis for nonlinear bounded-error estimation," *Automatica*, vol. 29, no. 4, pp. 1053–1064, 1993.

[13] S. Rump, *Developments in reliable computing*. Kluwer academic publisher, 1999, ch. IntLab – Interval laboratory, pp. 77–104.

[14] R. Malti, M. Aoun, F. Levron, and A. Oustaloup, "Analytical computation of the H_2-norm of fractional commensurate transfer functions," *Automatica*, vol. 47, no. 11, pp. 2425–2432, 2011.

[15] M. Tavazoei, "Notes on integral performance indices in fractional-order control systems," *Journal of Process Control*, vol. 20, no. 3, pp. 285 – 291, 2010. [Online]. Available: http://www.sciencedirect.com/science/article/B6V4N-4XHC6CK-1/2/20d020ac73210cb2ce6f0f6ab89e92e2